(41) Rasmussen, J. R.; Bergbreiter, D. E.; Whitesides, G. M. *J. Am. Chem. Soc.* **1977**, *99*, 4746.
(42) Gerenser, L. J.; Elman, J. F.; Mason, M. G.; Pochan, J. M. *Polymer* **1985**, *26*, 1162.
(43) Everhart, D. S.; Reilley, C. N. *Surf. Interface Anal.* **1981**, *3*, 126.
(44) Everhart, D. S.; Reilley, C. N. *Surf. Interface Anal.* **1981**, *3*, 258.
(45) Ikada, Y.; Matsunaga, T.; Suzuki, M. *Nippon Kagaku Kaishi* **1985**, *6*, 1079.
(46) Chapter 2 of ref 3 contains an excellent discussion of polymer structure, relaxations, and transitions in regard to polymer surface dynamics.
(47) Dias, A. J.; McCarthy, T. J. *Macromolecules* **1985**, *18*, 1826.
(48) Dias, A. J.; McCarthy, T. J. *Macromolecules* **1987**, *20*, 2068.
(49) Lee, K.-W.; McCarthy, T. J. *Macromolecules* **1987**, *20*, 1437.
(50) Lee, K.-W.; McCarthy, T. J. *Macromolecules* **1988**, *21*, 2318.
(51) Lee, K.-W.; McCarthy, T. J. *Macromolecules* **1987**, *21*, 3353.
(52) In several experiments that involved gravimetric analysis[47,48] we noted that drying film samples to constant mass at elevated temperatures (which were required) affected contact angle and/or XPS results and these measurements had to be made prior to complete drying.
(53) Any residual strain in PCTFE film is likely unimportant with regard to the experiments reported here. The fact that certain samples are stable with respect to thermal treatment indicates that residual strain is not responsible for surface reconstruction. The modification reactions and particularly the swelling of the modified surfaces by the reaction solutions significantly restructure the surface so that any residual strain incorporated in the surface region during processing is removed.
(54) These calculations use the value of 14 Å for the mean free path of $C_{1s}$ electrons excited with Mg K$\alpha$ irradiation. This value was measured in poly(*p*-xylylene): Clark, D. T.; Thomas, H. R. *J. Appl. Polym. Sci., Polym. Chem. Ed.* **1977**, *15*, 2843.
(55) The volumes of PCTFE and PCTFE-TMO repeat units were calculated to be 92 and 258 Å$^3$, respectively, using the density of PCTFE (2.1 g/cm$^3$) and assuming a density of 1.0 g/cm$^3$ for PCTFE-TMO. The figure is drawn to represent cross sections of spheres with these volumes (diameters of 5.6 and 7.9 Å).
(56) Receding contact angle ($\theta_R$) changes parallel the $\theta_A$ changes; $\theta_R$ data were generally more scattered than those for $\theta_A$.
(57) This experiment is also evidence that PCTFE-TMO groups remain attached during annealing. The XPS results and UV-vis spectroscopy also support this.

**Registry No.** PCTFE, 9002-83-9; TMO, 1772-43-6.

# Kinetics of the Gas-Phase Halogenation of a Polyethylene Surface As Studied with X-ray Photoelectron Spectroscopy

**James F. Elman,† Louis J. Gerenser,* Kim E. Goppert-Berarducci, and John M. Pochan**

*Research Laboratories, Eastman Kodak Company, Rochester, New York 14650*

*Received November 13, 1989*

ABSTRACT: X-ray photoelectron spectroscopy (XPS) has been used to determine the kinetics of gas-phase halogenation of a polyethylene surface. XPS allows the determination of the concentration of each carbon species present based upon chemical bonding. With this information detailed information about the kinetics has been obtained. The gas-phase chlorination of polyethylene was shown to follow predictable kinetics based on the XPS results. A time distribution of the monochlorinated and dichlorinated species was found, with the monochlorinated species more predominant. Chlorination kinetics are shown to predictably proceed for up to 600-s exposure to chlorine gas. At this exposure a $CH_2/CHCl/CCl_2$ ratio of 1/1/0.5 was found. For exposures >600 s, chlorination slows drastically. It is postulated that this latter effect is due to steric effects. Angular-dependent XPS data have shown that chlorination of polyethylene is uniform throughout the sampling depth (~10–70 Å). The XPS results suggest the bromination kinetics are also first order but ~$10^5$ slower than that of chlorination. The rate of iodination was found to be orders of magnitude slower than that of bromination.

## Introduction

Polymer surface properties control wettability,[1] adhesion,[1] and in some cases electronic properties.[2] These properties are many times altered via chemical modification of the surface. This modification can be made via chemical reaction with a contacting solution,[3,4] corona discharge treatment (CDT),[5,6] plasma or glow discharge treatment,[7,8] gas-phase reactions,[5,6] and combinations of the aforementioned treatments.[9] We have investigated the effects of CDT on polymer surfaces and the physisorption of surfactant molecules on the treated surfaces.[10,11] The chemistry involved in CDT treatment is complicated, with a series of hydrophilic chemical moieties created. These structures are dependent upon treatment power and treatment atmosphere and have been analyzed by gas-phase derivatization followed by XPS. In order to understand more completely the effect of gas-phase reactions on polymer surfaces, the gas-phase halogenation of polyethylene has been studied. XPS can be used to identify the various chemical species formed in the surface region (~10–70 Å) and can differentiate a chemical gradient within this region. It is the purpose of this study to (1) ascertain if the kinetics of formation of the various chemical species can be modeled and (2) determine whether this study can verify the selective chlorination kinetics observed by others.[12-14] These latter studies indicate that a halogenated carbon atom greatly affects the halogenation of an adjacent atom.

## Experimental Section

The XPS spectra were obtained on either a Hewlett-Packard 5950A or a Surface Science Laboratories SSX-100 photoelectron spectrometer, both of which have monochromatic Al K$\alpha$ X-ray sources (1486.6 eV). The use of a monochromatic source minimizes sample radiation damage, which is especially important

† Present address: University of Connecticut, Storrs, CT 06269.

0024-9297/90/2223-3922$02.50/0 

for polymers. All samples were analyzed at ambient temperature and exhibited no evidence of X-ray damage during analysis. The pressure in the spectrometer during analysis was typically $2 \times 10^{-9}$ Torr. Unless otherwise noted, all samples were analyzed at an electron takeoff angle (ETOA) of 38°, which corresponds to an analysis depth of ~50 Å (98% of the photoelectron signal orginates from a depth of $3\lambda$, where $\lambda \sim 25$ Å for 1200-eV electrons in a polymer matrix).[15] All angular-dependent measurements were made on the Hewlett-Packard instrument by using a Surface Science Laboratory Model 259 angular-rotation probe and by altering the magnification of the four-element electron lens from −5.0 to −2.3. This reduces the electron acceptance solid angle of the electron lens from a 3.5° to a 2.8° half-angle cone.

Typically, the full-width at half-maximum (fwhm) for the C 1s peak in a clean polyethylene sample varied from 0.9 to 1.0 eV. After halogenation, the fwhm of the individual components of the C 1s spectrum increased to 1.2–1.6 eV. The distribution of the various halogenated carbon species was determined with a line-shape analysis routine utilizing a 90% Gaussian/10% Lorentzian line shape for the individual peaks. The fwhm values of the peaks due to the halogenated carbon species were constrained to values between 1.2–1.4 eV depending on the level of halogenation, while the peak due to the unreacted carbon was left unconstrained. To confirm the validity of the line-shape analysis, the chlorine concentration, as determined from the integrated area under a chlorine core-level peak (both the Cl 2s and Cl 2p peaks were analyzed and provided identical results) after correction for ionization cross section, was compared to the values calculated on the basis of the line-shape analysis of the C 1s peak. The two methods provided agreement within 5%. Since both chlorine core-level peaks and the C 1s peak are relatively close in kinetic energy (1286 and 1217 eV vs 1202 eV), no correction was made for differences in electron inelastic mean-free path.

The polyethylene samples were commercial 4-mil high-density polyethylene. The samples were cleaned with repetitive washings of acetone, isopropyl alcohol, and distilled water. Halogenation reactions were carried out in a specially designed glass gas bubbler apparatus. After the polyethylene sample was placed in the reaction vessel, the vessel was purged with nitrogen and then the appropriate gas (chlorine or bromine) was released into the vessel. For chlorination, a chlorine gas lecture cylinder (Air Products Speciality Gases, purity 99.5%) was attached to the reaction vessel. Bromination was accomplished by putting a small bottle containing bromine liquid (Aldrich) in the reaction vessel along with the polyethylene sample and allowing the polyethylene to remain exposed to the bromine vapor. At the end of the reaction time, the gas flow was stopped and the system was again purged with nitrogen. The halogenated polyethylene was then inserted into the preparation chamber of the spectrometer where it was evacuated to a pressure of $\sim 5 \times 10^{-9}$ Torr. The halogenated polyethylene was allowed to remain in the preparation chamber for several hours before analysis. This was done to remove any physisorbed gas or volatile short-chain species that may have been produced by the halogenation reaction.

## Results and Discussion

A free-radical kinetics scheme for the halogenation of polyethylene is outlined in Figure 1. The initiation step involves the breakdown of a halogen molecule into a free radical. The propagation reactions then proceed until the termination steps result in the consumption of all of the reactive species. Experimental evidence (see below) has shown that, in this sequence of reactions, the −CHX− species forms much faster than the $-CX_2$ species. The following assumptions were made in order to simplify the kinetics:

(1) Reactions containing $k_4$ and $k_8$ are essentially zero since very little HX would remain in the reaction media.

(2) Reactions involving $k_{11}$ and $k_{13}$ are approximately zero. These are cross-linking reactions, and we do not have any experimental evidence of cross-linking occurring. Also the probability of two free radicals reacting is minimal because of their low concentration.

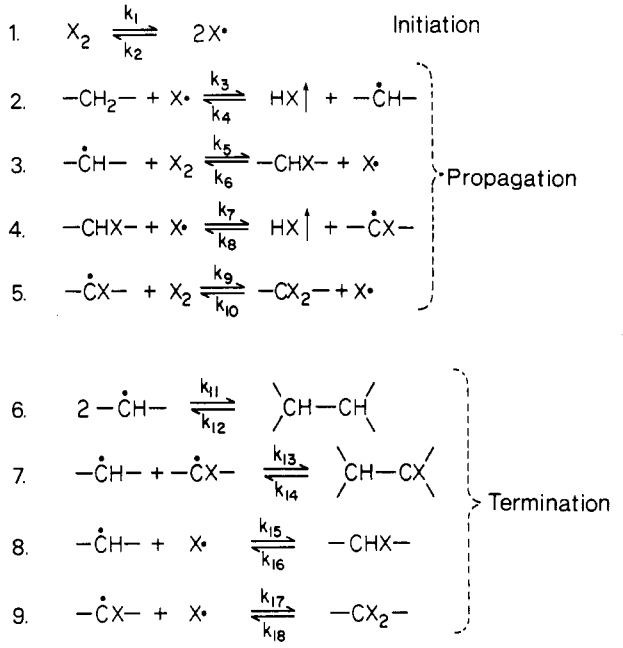


**Figure 1.** Proposed free-radical reaction scheme for the halogenation of polyethylene.

(3) Reactions 8 and 9 are negligible. The probability of two radicals reacting with each other is very small, and the process of free-radical formation by dissociation of a halogenated hydrocarbon should be less than halogen dissociation.

(4) There exists a steady-state concentration of the halogen free radical; i.e., $dX/dt = 0$.

(5) There exists a steady-state concentration of the $-C^{\bullet}H-$ free radical; i.e., $d[-C^{\bullet}H-]/dt = 0$.

(6) $k_5 \gg k_6$. There is no driving force for the reverse reaction to occur.

(7) $k_9 \gg k_7$. The rate of formation of $-C^{\bullet}X-$ controls $-CX_2-$ formation.

**Chlorination ($t \leq 600$ s).** Survey scans for a polyethylene surface before and after a 10-min exposure to chlorine gas are shown in Figure 2. Note the absence of any contaminants for both surfaces. For the clean polyethylene surface, one peak (C 1s) at a binding energy of 284.6 eV is observed. After chlorination, two new peaks are observed at binding energies of 200 and 270 eV due to the Cl 2p and Cl 2s levels, respectively. High-resolution scans of the C 1s region are shown in Figure 3. The C 1s region of a clean polyethylene sample is shown in Figure 3a. The neutral or unreacted carbon peak at 284.6 eV is the only carbon peak that is observed. After a 15-s exposure to chlorine gas, the emergence of a second peak at a higher binding energy (286.0 eV) is evident in the C 1s spectrum (Figure 3b). This peak is assigned to −CHCl−. The chlorine concentration at this exposure level is 6.5%. After a 2-min exposure to chlorine gas, a very prominent −CHCl− peak and an additional peak at a higher binding energy (287.4 eV) due to the formation of $-CCl_2-$ are observed (Figure 3c). The chlorine concentration has now increased to 37.5%. After 10 min, the −CHCl− peak is the predominant peak and the $-CCl_2-$ peak has approximately doubled in size (Figure 3d). The chlorine concentration is now 42.5%. The data are plotted as atomic percent of each species present versus time in Figure 4. This graph illustrates that there is a rapid initial decrease in unreacted carbon with a corresponding rapid increase in the monochlorinated species. The dichlorinated species increases at a much slower rate. Also, the monochlorinated species reaches a maximum after ~5 min

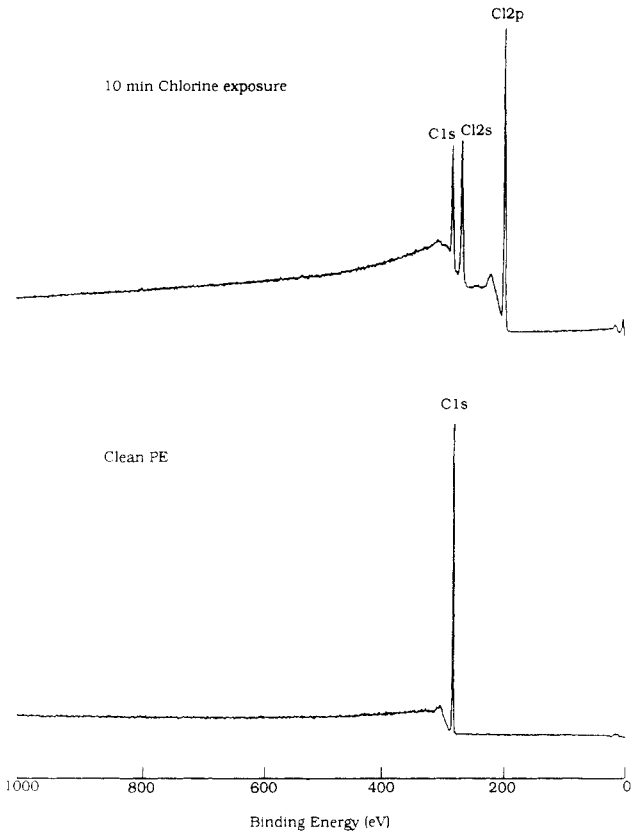


**Figure 2.** XPS survey scans for a polyethylene surface before and after 10-min exposure to chlorine gas.

and then begins to decrease whereas the dichlorinated species continues to increase. This is consistent with the conversion of some monochlorinated to dichlorinated species with increasing chlorine exposure. The following discussion will analyze each species (unreacted, monochlorinated, and dichlorinated carbon) separately for exposure times up to 600 s.

**Unreacted Carbon.** In order to study the kinetics of chlorination, the rate of change in concentration of each species with time must be determined. The change in unreacted carbon is examined first. From reaction 2 (Figure 1), the following expression is obtained for the change in concentration of $-CH_2-$ with time:

$$d[-CH_2-]/dt = k_3[-CH_2-][Cl^\bullet] \quad (1)$$

If the concentration of free radicals is constant (assumption 4), then the concentration of free radical can be included in $k_3$; i.e.

$$d[-CH_2-]/dt = k'_3[-CH_2-] \quad (2)$$

Equation 2 can be integrated to provide eq 3, which indicates a first-order decrease in unreacted carbon with time

$$[-CH_2-] = [-CH_2-]_0 e^{-k'_3 t} \quad (3)$$

A plot of this equation as the log concentration of unreacted carbon minus a constant versus time is shown in Figure 5. The constant is due to the fact that even with long reaction times not all of the carbon atoms react with a chlorine atom. Solving for $k'_3$ gives a value of $1.5 \times 10^{-2}$ $s^{-1}$ for this rate constant. The excellent correlation obtained from this equation suggests that the reaction is simple first order. The data can also be plotted as the atomic percent of unreacted carbon versus time as in Figure 6. The solid squares are the experimental points, and the solid line is the theoretical curve obtained using eq 3. The

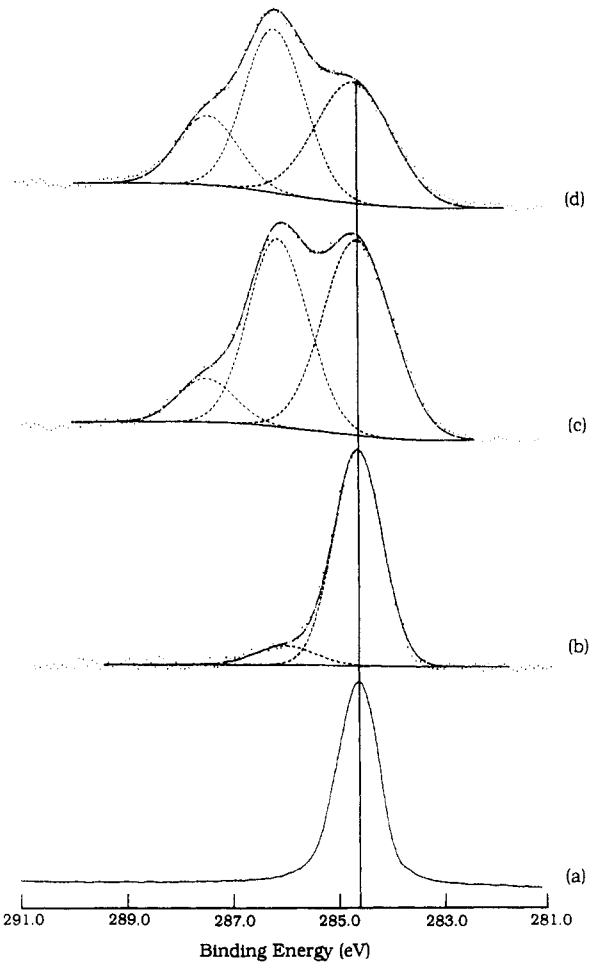


**Figure 3.** XPS C 1s spectra for (a) clean polyethylene, (b) 15-s chlorination, (c) 2-min chlorination, and (d) 10-min chlorination.

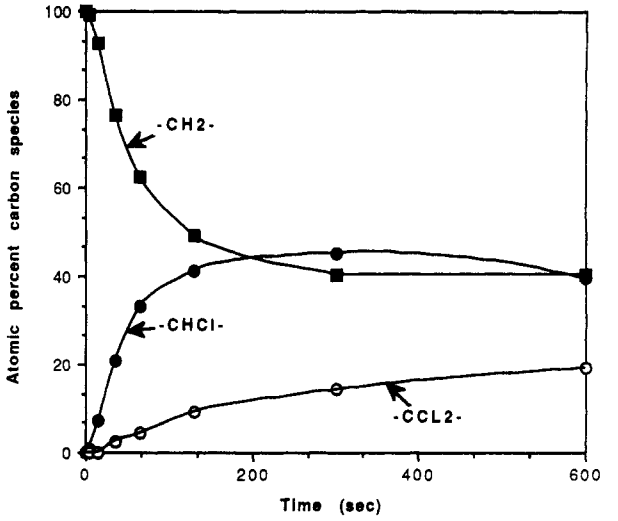


**Figure 4.** Concentration of individual carbon species as a function of chlorination time.

correlation between the two is excellent. When plotted in this manner, it is readily apparent that ~40% of the carbon atoms do not react even at long reaction times. The time-dependent concentration of $[-CH_2-]$ thus becomes

$$[-CH_2-] = 40.4 + 59.6e^{-k'_3 t} \quad (4)$$

There are, at least, three possible explanations for the unreacted carbon:

(1) Nonuniform halogenation within the sampling depth of XPS. This possibility has been eliminated since angular-dependent XPS studies have shown that within the

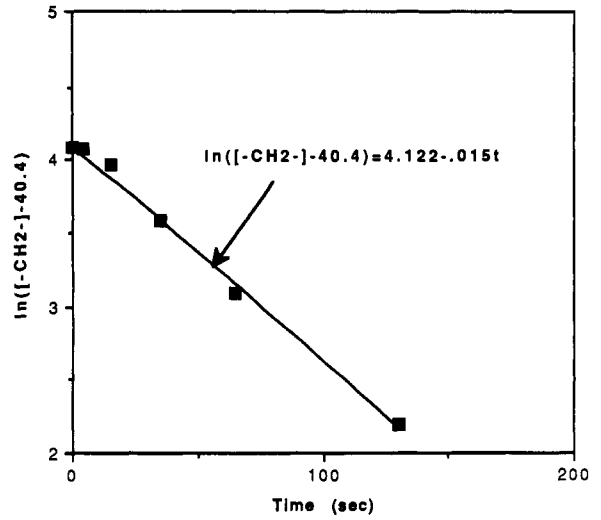


**Figure 5.** ln (unreacted carbon − constant) as a function of chlorination time.

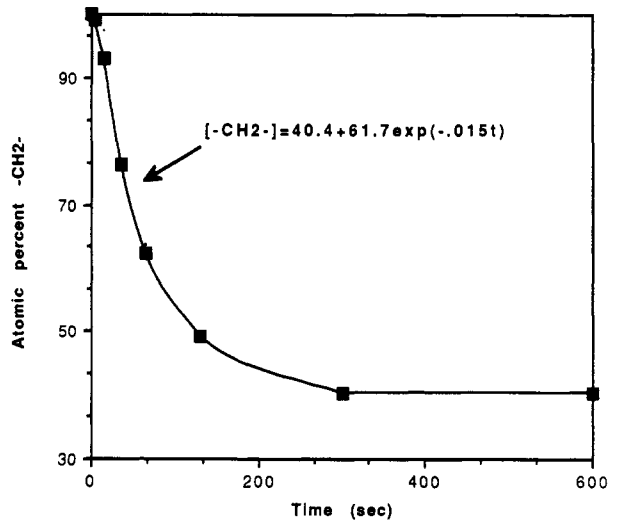


**Figure 6.** Unreacted carbon concentration as a function of chlorination time. Squares are experimental data points, and the solid line is the theoretical curve obtained from eq 2.

sampling depth there is a uniform chlorine treatment. The results of several angular-dependent XPS experiments are shown in Figure 7. Two different chlorination times were used, a 30-s and a 2-min exposure. The measurements for the 2-min sample were carried out over several days whereas the 30-s experiment was completed in several hours. The slight decrease noted in the 2-min sample may be due to the loss of chlorine with time. It was noted in earlier chlorination experiments that there was a rapid initial loss of chlorine with a slower loss over several hours and days. The initial decrease in chlorine concentration may be due to the loss of short-chain species via diffusion or sublimation from the surface while the slower decrease might be the result of either migration of low molecular weight species and/or surface reorganization. The 30-s unannealed data suggest a slight increase in the Cl/C ratio at higher electron take-off angles. The change is, however, very slight and at a relatively low chlorine concentration is within experimental error. The 30-s annealed sample was similarly exposed to chlorine gas but was then heated at 50 °C in the preparation chamber overnight. This was done to promote an equilibrium state with respect to chlorine loss before analysis since heat treatment was found to speed up the decrease in the chlorine concentration at the surface noted earlier. All the kinetic experiments were carried out at the standard electron take-off angle of 38°,

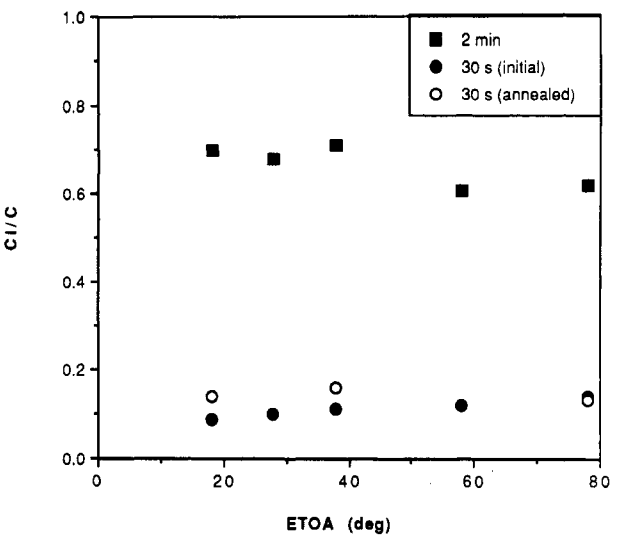


**Figure 7.** Angular-dependent XPS data for chlorinated polyethylene. The data at the lowest electron take-off angle (ETOA) is the most surface sensitive.

which samples approximately the first 50 Å. The angular-dependent XPS experiments indicate that the chlorination treatment is uniform within this depth.

(2) Polyethylene crystallinity. Polyethylene is normally about 68% crystalline. Any carbon atoms in this crystalline region should not be accessible to halogenation and should not react. Based solely on crystallinity, the data in Figure 6 and 7 suggest that, within the XPS sampling depth, polyethylene is about 40% crystalline.

(3) Steric hindrance. We feel that this is the most plausible reason for the unreacted carbon atoms. Other workers have observed a similar extent of unreacted carbon in the bulk, which they attribute to steric factors.[12-14] Based on steric hindrance, the XPS data suggest that adjacent carbon atoms can be monochlorinated; however, dichlorination can only occur on carbon atoms adjacent to neutral or unreacted carbon atoms.

**Monochlorinated Carbon Formation.** We assume that the rate of formation of –CHCl– is rate limited by the formation of –C•H–; i.e., $k_5 \gg k_3$. Considering reactions 2–4 (Figure 1), the following kinetic equations can be written.

$$d[\text{–CHCl–}]/dt = k_5[Cl_2][\text{–C•H–}] - k_7[\text{–CHCl–}][Cl^\bullet] \quad (5)$$

If the concentration of [–C•H–] is considered constant (steady-state approximation), the following equation can be written:

$$d[\text{–C•H–}]/dt = k_3[\text{–CH}_2\text{–}][Cl^\bullet] - k_5[\text{–C•H–}][Cl_2] = 0 \quad (6)$$

Therefore

$$[\text{–C•H–}] = k_3[\text{–CH}_2\text{–}][Cl^\bullet]/k_5[Cl_2] \quad (7)$$

Substituting into eq 5 provides

$$d[\text{–CHCl–}]/dt = k_5[Cl_2](k_3[\text{–CH}_2\text{–}][Cl^\bullet]/k_5[Cl_2]) - k_7[\text{–CHCl–}][Cl^\bullet] \quad (8a)$$

$$= k_3[\text{–CH}_2\text{–}][Cl^\bullet] - k_7[\text{–CHCl–}][Cl^\bullet] \quad (8b)$$

The time dependence of [–$CH_2$–] has already been determined (eq 3) and can be substituted to provide

$$d[\text{–CHCl–}]/dt = k_3[\text{–CH}_2\text{–}]_0 e^{-k'_3 t}[Cl^\bullet] - k_7[\text{–CHCl–}][Cl^\bullet] \quad (9)$$

Since the concentration of [Cl•] is assumed to be constant,

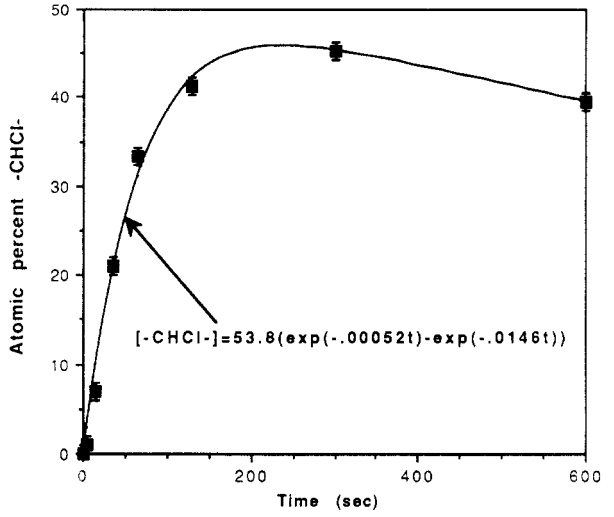


**Figure 8.** -CHCl- concentration as a function of chlorination time. Squares are experimental data points, and the solid line is the theoretical curve obtained from eq 7.

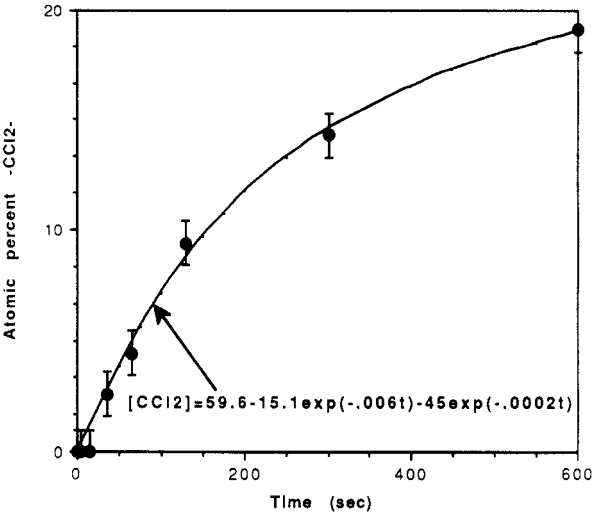


**Figure 9.** $-CCl_2-$ concentration as a function of chlorination time. Circles are experimental data points, and the solid line is the theoretical curve obtained from eq 14.

eq 9 can be written as

$$d[-CHCl-]/dt = k'_3[-CH_2-]_0 e^{-k'_3 t} - k'_7[-CHCl-] \quad (10)$$

Solving the above provides

$$[-CHCl-] = A[e^{-k'_7 t} - e^{-k'_3 t}] \quad (11)$$

A nonlinear regression of -CHCl- versus time data provides the values of $1.5 \times 10^{-2}$ and $5.2 \times 10^{-4}$ $s^{-1}$ for $k'_3$ and $k'_7$, respectively. The value of $k'_3 = 1.5 \times 10^{-2}$ $s^{-1}$ is identical with that previously obtained for the unreacted carbon rate constant. If this equation is then plotted as atomic percent -CHCl- versus time, the graph shown in Figure 8 is obtained. Again, there is excellent correlation between the experimental and theoretical data.

**Dichlorinated Carbon Formation.** Finally, the kinetics of the dichlorinated species, $-CCl_2-$, can be determined. However, in order to do this another assumption must be made: that a concentration gradient does not exist within the XPS sampling depth. The angular-dependent XPS results discussed previously suggest that this assumption is valid. Accepting this assumption as correct provides the following:

$$[-CH_2-] + [-CHCl-] + [-CCl_2-] = C \quad (12)$$

That is, the sum of the various carbon species is a constant. Solving for $[-CCl_2-]$ provides

$$[-CCl_2-] = C - [-CH_2-] - [-CHCl-] \quad (13)$$

Then substituting the appropriate values in eqs 3 and 11 gives the following equation:

$$[-CCl_2-] = C - [-CH_2-]_0 e^{-k'_3 t} - A[e^{-k'_7 t} - e^{-k'_3 t}] \quad (14)$$

A nonlinear regression of eq 14 with experimental data provides $k'_3$ and $k'_7$ values of $0.6 \times 10^{-2}$ and $1.9 \times 10^{-4}$ $s^{-1}$, respectively.

A plot of the experimental data compared with the theoretical fit determined from eq 14 is shown in Figure 9. Note the excellent correlation between experimental and theoretical data. The values obtained for the rate constants based on the $CCl_2$ kinetics are significantly different from those derived from the other kinetic fits. This is probably due to (1) our assumption concerning a homogeneous distribution of the various carbon species within the XPS sampling depth is not valid or (2) the fact that the total amount of dichlorinated species measured is relatively small compared to the monochlorinated and unreacted species. The concentration of -CHCl- ranged between 0 and 45.3% whereas the maximum amount of $-CCl_2-$ measured is 19.1%. Thus slight errors in the $-CCl_2-$ concentration are magnified to a greater extent in a regression analysis. Suffice it to say that the fit is well within the error limits of the measurement.

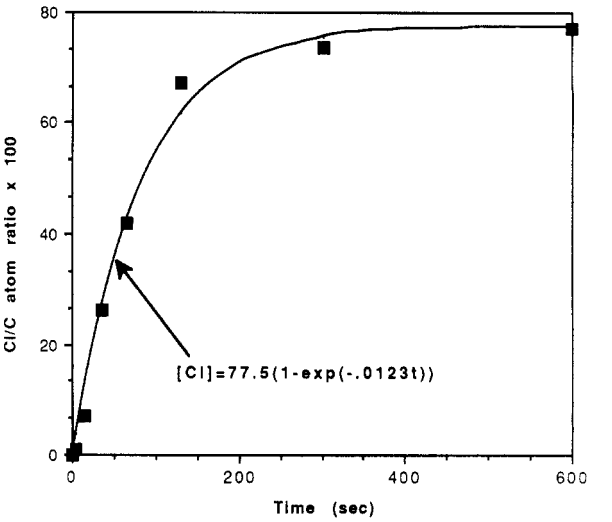


**Figure 10.** Chlorine/carbon atom ratio as a function of chlorination time. The squares are the experimental data points, and the solid line is a linear regression of the data.

The value of XPS for this analysis is clearly demonstrated if the following analysis is considered. If only the total carbon and chlorine content of the films studied had been monitored, the data would appear as in Figures 6 and 10. The chlorine concentration versus time is plotted in Figure 10. Again a plateau is reached, indicating that only a certain amount of chlorine can be incorporated into the polyethylene. Note the excellent agreement between theory and experimental results. Both plots suggest classical first-order kinetic behavior. XPS, however, provides a method of determining the amount of each species present. With this information, the total kinetic picture of chlorination evolution is determined.

In the above analysis, no consideration is given to the effect of neighboring halogenated carbon atoms on the kinetics of halogenation of unreacted carbon atoms.[12-14] It is interesting to note that the polyethylene surface is considered homogeneous with all carbon atoms identical. A simple kinetic picture can explain the experimental data,

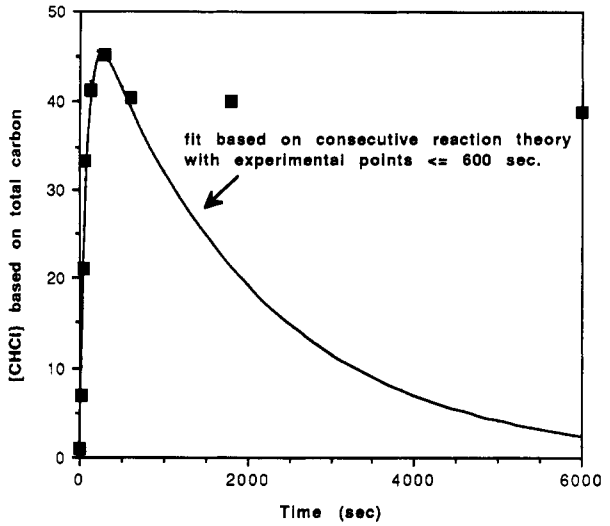


**Figure 11.** Comparison of predicted (solid line) and experimental (squares) behavior of -CHCl- concentration for long exposure times ($t$ > 600 s).

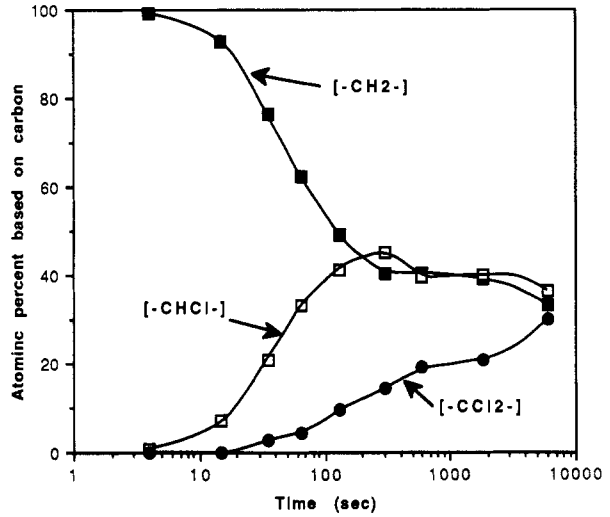


**Figure 12.** Long exposure time ($t$ > 600 s) behavior of individual carbon species.

except for the ~40% unreacted carbon atoms. The data at $t$ = 600 s indicate a $CH_2/CHCl/CCl_2$ ratio of 1/1/0.5. Based on stoichiometry, the XPS data suggest that adjacent carbon atoms can be monochlorinated; however, dichlorination can only occur on carbon atoms adjacent to unreacted carbon atoms.

**Chlorination ($t$ > 600 s).** For chlorination times greater than 600 s, the formation of the various species does not continue as predicted by the kinetics established at shorter times. This is shown in Figure 11 where the theoretical (based on the kinetics determined at $t \leq 600$ s) and actual CHCl concentrations are plotted. The time dependence of all species is plotted in Figure 12 where it is shown that the chlorination continues but at a much slower rate after 600-s exposure. The data in Figure 13 indicate that the $CH_2$ disappearance is still first order, but with a rate constant approximately 3 orders of magnitude less than before.

There are several possible explanations for such behavior: (1) steric hindrance, (2) polyethylene crystallinity, (3) limited chlorine solubility in the highly chlorinated polyethylene, and (4) a glass transition ($T_g$) effect limiting chlorine diffusion. Possibilities (1) and (2) have been discussed previously. The glass transition effect can be eliminated as follows: if the $T_g$ of solution-chlorinated polyethylene is determined as a function of

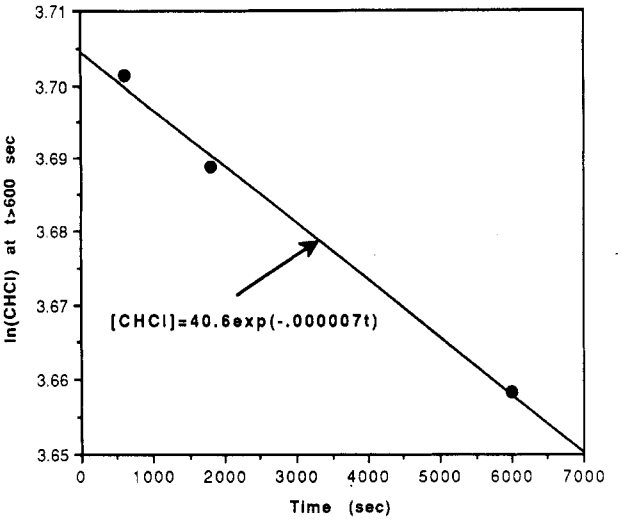


**Figure 13.** ln [-CHCl-] behavior for long exposure times ($t$ > 600 s).

chlorine content, it varies monotonically from ~−80 °C for polyethylene to ~180 °C for a Cl/C ratio of 0.9.[16] The gas-phase reaction is observed to slow down at a Cl/C ratio of ~0.8. This value corresponds to a $T_g$ of ~100 °C for solution-chlorinated polyethylene. If $T_g$ were controlling the gas-phase reaction, it would be expected to continue predictably only to a Cl/C ratio that provides ambient $T_g$. This value is ~0.4.

The limited solubility of chlorine gas cannot be eliminated as a possible cause of the observed effect; however, the solubility change should be gradual and the assumptions concerning the constant chlorine free-radical population would be invalid in the kinetic derivations. This is not the case for fits of the data up to 600-s exposure. We believe that steric hindrance limits the chlorination behavior. Krentsel and co-workers[17] have shown with solution chlorination of polyethylene that chlorination hinders further addition of chlorine atoms at adjacent sites to that of the original chlorinated site. This does not appear to be the case in our gas-phase chlorination since the kinetic model assumes no specificity and fits the data.

**Bromination.** Bromination of polyethylene proceeds at a much slower rate than chlorination. The results of bromination are shown in Figure 14. Even after 11 days ($1.7 \times 10^4$ min), the bromine concentration at the surface is only slightly greater than 12%. The rate constant, $k'_3$, for bromination was determined only from the atomic percent change in unreacted carbon since the concentration of the individual brominated species was too low to measure accurately. The value for $k'_3$ is $1.4 \times 10^{-7}$ $s^{-1}$, 5 orders of magnitude lower than the values obtained for chlorination. Table I summarizes the rate constants for chlorination and bromination.

It should be noted that the bromination rate for polyethylene, although analyzed similarly to chlorination, appears more complicated. If the data in Figure 14 are examined carefully, a rapid uptake in bromine is initially observed. This is followed by a slower rate. The size of the bromine atom is larger than that of chlorine, and surface uptake could be much more facile than subsurface uptake. This premise is currently being explored.

**Iodination.** A polyethylene sample was exposed to iodine vapors for 141 days in a sealed glass container containing iodine crystals. Before XPS analysis, the polyethylene was removed from the container and left exposed to atmosphere for 24 h to remove any phys-

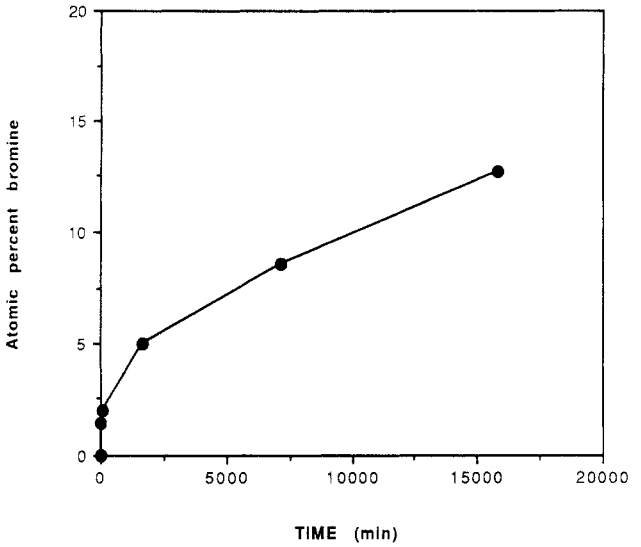


**Figure 14.** Bromine concentration as a function of bromination time.

**Table I**
**Summary of Rate Constants Determined from the XPS Data**

Chlorination ($t \leq 600$ s)

1. $[-CH_2-] = 40.4 + 59.6e^{-k'_3 t}$
   $k'_3 = 1.5 \times 10^{-2}$ s$^{-1}$
2. $[-CHCl-] = A(e^{-k'_7 t} - e^{-k'_3 t})$
   $k'_3 = 1.5 \times 10^{-2}$ s$^{-1}$
   $k'_7 = 5.2 \times 10^{-4}$ s$^{-1}$
3. $[-CCl_2-] = C - [-CH_2-]_0 e^{-k'_3 t} + A(e^{-k'_7 t} - e^{-k'_3 t})$
   $k'_3 = 0.6 \times 10^{-2}$ s$^{-1}$
   $k'_7 = 1.9 \times 10^{-4}$ s$^{-1}$

Bromination

1. $[-CH_2-] = [-CH_2-]_0(e^{-k'_3 t} + 17)$
   $k'_3 = 1.4 \times 10^{-7}$ s$^{-1}$

isorbed iodine. The polyethylene was than mounted in the preparation chamber of the spectrometer ($\sim 10^{-8}$ Torr) for 5 h before analysis. The total amount of iodine determined from the XPS analysis was 0.34%. This is as expected since one would expect the kinetics of iodination to be orders of magnitude slower than that observed for bromination.

## Conclusions

XPS has been shown to be very useful in determining the kinetics of halogenation of a polyethylene surface. Without the information obtained from the XPS results, chlorination appears to proceed via relatively simple first-order kinetics. XPS allows the determination of the concentration of each carbon species present based upon chemical bonding. With this information much more detailed information about the kinetics can be obtained. After such analysis, the gas-phase chlorination of polyethylene was shown to follow more complicated predictable kinetics. A time distribution of the monochlorinated and dichlorinated species exists, with the monochlorinated species more predominant. For chlorination times greater than 600 s, the kinetics were found to slow markedly. Angular-dependent XPS data have shown that chlorination of polyethylene is uniform throughout the XPS sampling depth. Within this depth, about 60% of the carbon atoms are rapidly chlorinated. The unreacted carbon atoms are assumed either to be in a crystalline environment or to be inaccessible due to steric hindrance. The XPS results suggest that the bromination kinetics are also first order but $\sim 10^5$ slower than that of chlorination. The rate of iodination was found to be orders of magnitude slower than that of bromination and was not studied in detail.

## References and Notes

(1) Wu, S. *Polymer Interface and Adhesion*; Marcel Dekker: New York, 1982.
(2) Pochan, J. M.; Gibson, H. W.; Bailey, F. C.; Hinman, D. F. *J. Electrost.* **1980**, *8*, 183.
(3) Batich, C. D. *Appl. Surf. Sci.* **1988**, *32*, 57.
(4) Lee, K.; McCarthy, T. *Polym. Prepr.* **1988**, *29*, 334.
(5) Pochan, J. M.; Gerenser, L. J.; Elman, J. F. *Polymer* **1986**, *27*, 1058.
(6) Gerenser, L. J.; Elman, J. F.; Mason, M. G.; Pochan, J. M. *Polymer* **1985**, *26*, 1192.
(7) Gerenser, L. J. *J. Vac. Sci. Technol.* **1988**, *6* (5), 2897.
(8) Gerenser, L. J. *J. Adh. Sci. Technol.* **1987**, *1* (4), 303.
(9) Grimm, H. J.; Thomas, E. L. *Polymer* **1985**, *26*, 27.
(10) Gerenser, L. J.; Pochan, J. M.; Elman, J. F.; Mason, M. G. *Langmuir* **1986**, *2*, 765.
(11) Gerenser, L. J.; Pochan, J. M.; Mason, M. G.; Elman, J. F. *Langmuir* **1985**, *1*, 305.
(12) Mikhailovm, M.; Stoeva, S. *God. Vissh. Khim.-Tekhnol. Inst. "Prof. d-r As. Zlatarov", gr. Burgas*, **1976**, *1*, 205.
(13) Noa, O. V.; Litmanovich, A. D. *Vysokomol. Soedin., Ser. A* **1977**, *19*, 1211.
(14) Krentsel, L. B.; Litmanovich, A. D.; Pastukhova, I. V.; Agasanoyan, V. A. *Vysokomol. Soedin., Ser. A* **1971**, *13*, 2489.
(15) Roberts, R. F.; Allara, D. L.; Pryde, C. A.; Buchanan, D. N. E.; Hobbins, N. D. *Surf. Interface Anal.* **1980**, *2*, 5.
(16) Ulrich, H. *Introduction to Industrial Polymers*; Macmillan, New York, 1982.
(17) Krentsel, L. B.; Litmanovich, A. D.; Pastukhova, I. V.; Agasanoyan, V. A. *Vysokomol. Soedin., Ser. B* **1969**, *11* (12), 829.

**Registry No.** Polyethylene, 9002-88-4.